### Emergent phases in a compass chain with multi-site interactions

Wen-Long You, <sup>1</sup> Cheng-Jie Zhang, <sup>1</sup> Weihai Ni, <sup>1</sup> Ming Gong, <sup>2</sup> and Andrzej M. Oleś<sup>3,4</sup>

<sup>1</sup>College of Physics, Optoelectronics and Energy, Soochow University, Suzhou, Jiangsu 215006, P.R. China
<sup>2</sup>Key Laboratory of Quantum Information and Synergetic Innovation Center of Quantum Information and Quantum Physics,
University of Science and Technology of China, Hefei, Anhui 230026, P.R. China
<sup>3</sup>Max Planck Institute for Solid State Research, Heisenbergstrasse 1, D-70569 Stuttgart, Germany
<sup>4</sup>Marian Smoluchowski Institute of Physics, Jagiellonian University, prof. S. Łojasiewicza 11, PL-30348 Kraków, Poland
(Dated: October 5, 2018)

We study a dimerised spin chain with biaxial magnetic interacting ions in the presence of an externally induced three-site interactions out of equilibrium. In the general case, the three-site interactions play a role in renormalizing the effective uniform magnetic field. We find that the existence of zero-energy Majorana modes is intricately related to the sign of Pfaffian of the Bogoliubov-de Gennes Hamiltonian and the relevant  $Z_2$  topological invariant. In contrast, we show that an exotic spin liquid phase can emerge in the compass limit through a Berezinskii-Kosterlitz-Thouless (BKT) quantum phase transition. Such a BKT transition is characterized by a large dynamic exponent z=4, and the spin-liquid phase is robust under a uniform magnetic field. We find the relative entropy and the quantum discord can signal the BKT transitions. We also uncover a few differences in deriving the correlation functions for the systems with broken reflection symmetry.

### PACS numbers: 73.21.-b,71.10.Pm,78.40.Kc

#### I. INTRODUCTION

Several intriguing phenomena in condensed matter systems originate from the interplay of strong electron correlations and frustration. Frustration occurs intrinsically in the systems with degenerate and partly occupied orbitals. A representative model which stands for the orbital-orbital interactions in Mott insulators is the so called two-dimensional (2D) compass model [1] where nearest neighbor interactions like  $\propto \sigma_i^\alpha \sigma_j^\alpha$  (with  $\alpha = x, z$  being spin component) compete with each other along two different spatial directions of the bonds. In such a frustrated quantum system, the spins cannot order simultaneously to minimize all local interactions, and the ground state is highly degenerate.

The dominating finite-range interactions in many-body systems can lead to the onset of self-ordered phases in spin systems. One-dimensional (1D) quantum models are natural playgrounds for hosting different orders and distinct universality, especially some exactly solvable models such as the 1D compass model [2]. Here again the competing interactions are between nearest neighbors. However, the range of the hybridization of the electron wave function will be more extended in reality than only to nearest neighbor sites in some realistic bonding geometries, such as CsCoCl<sub>3</sub> [3], LiCu<sub>2</sub>O<sub>2</sub> [4, 5], NaCu<sub>2</sub>O<sub>2</sub> [6]. The ramifications are that longer-range interactions should be taken into account. Complex interactions including the three-spin interactions between three consecutive sites essentially enrich the ground state phase diagram of the spin model. Recently three-site interactions received considerable attention in a bit diverse context. It was realized that the three-site spin interaction can be included to exhibit the double ferroic order and multiferroics [7]. Experimentally, systems described by spin-1/2 Hamiltonians with three-spin interactions can be generated using optical lattices or in NMR quantum simulators [8–10].

So far, much attention has been focused on studies of spin-1/2 isotropic XY (or XX) model chains with two types of three-site interactions. One is the (XZX+YZY)-type of three-site interactions [11–16], where the exchange interaction for next nearest neighbor sites takes on XX form. The other form of three-site interactions is the (XZY-YZX) type [14–17]. It has been proven that the XX chain with the (XZX+YZY)-type of three-site interactions can be transformed to the one with the (XZY-YZX)-type and Dzyaloshinskii-Moriya (DM) interaction by a local spin rotation [11, 16].

On the other hand, a few works have been devoted to investigating the effects of three-site interactions for anisotropic XY chains, which can turn to Ising limit and XX limit by varying the anisotropy parameter. The three-site interactions include again either (XZX+YZY) [18–24] or (XZY-YZX) forms [24–28]. Differently from the situation on the XX chains, two kinds of three-site interactions on the XY chains are not unitary equivalent. The (XZX+YZY)-type interactions violate the time reversal (T) symmetry but preserve the parity (P) symmetry, while the (XZY-YZX)-type of three-site interactions break both symmetries simultaneously. Furthermore, a simplified version of three-site XZX interactions was also examined [29–32]. One finds that transverse Ising model with XZX-type interactions is dual to the XY model through a nonlocal dual transformation [33] which hosts a number of Majorana zero modes of an open chain [30].

The organization of the paper is as follows. In Sec. II we introduce the Hamiltonian of the 1D generalized compass model (GCM) with three-site interactions. Notation is introduced in Sec. II A and then we present the procedure to solve it exactly by employing Jordan-

Wigner transformation. Ground state properties and excited states are derived in Sec. IIB. Majorana modes and topological phase transition are addressed in Secs. IIC and IID. The exact solution explains the nature of the quantum phase transition (QPT) as explained in Sec. III. The model in the magnetic field is analyzed in Sec. IV. In Sec. V we discuss the aspects related to quantum information and present the fidelity susceptibility in Sec. V A and coherence susceptibility in Sec. V B. A final discussion and conclusions are presented in Sec. VI. More technical aspects of the presented solution are given in Appendices A and B.

#### II. THE MODEL AND ITS SOLUTION

### A. Generalized compass model in one dimension

The 1D GCM is a microscopic model to mimic zigzag spin chains in perovskite transition metal (TM) oxides. For instance,  $\mathrm{Co^{2+}}$  ions in  $\mathrm{CoNb_2O_6}$  compound form zigzag chains along the c axis. At low temperatures, Co spins orient themselves along two different easy axes in the nearly (a,c) plane with a 31° canting angle from the c axis. The Peierls-type spin-phonon coupling renders frustrated spin exchanges along distorted TM-O-TM bonds [34].

The 1D GCM with alternating exchange interaction considered below is given by [35–38],

$$\mathcal{H}_{GCM} = \sum_{i=1}^{N'} J_o \tilde{\sigma}_{2i-1}(\theta) \tilde{\sigma}_{2i}(\theta) + J_e \tilde{\sigma}_{2i}(-\theta) \tilde{\sigma}_{2i+1}(-\theta),$$

$$+ \sum_{i=1}^{N'} \left( \vec{h}_o \cdot \vec{\sigma}_{2i-1} + \vec{h}_e \cdot \vec{\sigma}_{2i} \right), \tag{1}$$

where the operator with a tilde sign is defined as a linear combinations of  $\{\sigma_i^x, \sigma_i^y\}$  pseudospin components,

$$\tilde{\sigma}_i(\theta) \equiv \cos(\theta/2)\,\sigma_i^x + \sin(\theta/2)\,\sigma_i^y.$$
 (2)

Here, N' = N/2 is the number of two-site unit cells.  $J_o(J_e)$  denotes the amplitude of the nearest-neighbor planar interaction on odd (even) bonds, while  $\vec{h}_o(\vec{h}_e)$  is the magnitude of the external field exerted on odd (even) sites. In addition, effective (XZX+YZY)-type three-site interactions are also taken into account,

$$\mathcal{H}_{3} = K \sum_{i=1}^{N} \left( \sigma_{i-1}^{x} \sigma_{i}^{z} \sigma_{i+1}^{x} + \sigma_{i-1}^{y} \sigma_{i}^{z} \sigma_{i+1}^{y} \right), \quad (3)$$

where K characterizes the strength of uniform exchange interaction between three consecutive spins. Multi-site interactions emerge simultaneously with two-body interactions as higher-order corrections in Mott insulating phases, but they are generally believed to have a negligible effect [39]. However, the experimental capability,

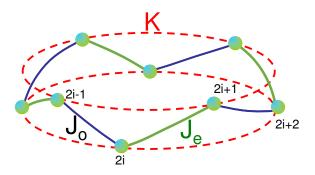


FIG. 1: Schematic representation of a zigzag spin chain with periodic boundary conditions described by the Hamiltonian Eq. (4). Nearest neighbor exchange interactions alternate between  $J_o$  (blue thin lines) and  $J_e$  (green thick lines) on odd and even bonds, respectively. K denotes three-site exchange parameter (red dashed lines).

such as cold atom technology, allows us to control three-spin interactions across a wide parameter range [40]. Remarkably, three-site interactions appear naturally as an energy current when a compass chain was in the nonequilibrium steady states [41, 42], which can be formally calculated by taking a time derivative of the energy density and follows from the continuity equation [43, 44]. Then the complete Hamiltonian of the 1D GCM with the three-site (XZX+YZY) interactions is,

$$\mathcal{H} = \mathcal{H}_{GCM} + \mathcal{H}_3. \tag{4}$$

Exchange couplings are shown schematically in Fig. 1. We shall mention that the combined model may be realized by quantum engineered artificial systems. For instance, coupling superconducting qubits to microwave circuitry provide a laboratory to simulate various spin models [45] and even multi-site interactions [46]. In particular, the cavity array can be driven and dissipative and thus be settled in a non-equilibrium steady state [32, 47]. As the simulated spin chain is driven out of equilibrium in the presence of an energy current, critical phase transitions between the pristine ground state and the current-carrying phase and the associated universality can be probed.

## B. Quasiparticles at finite three-site interactions and vanishing magnetic field

The Jordan-Wigner transformation maps explicitly the pseudospin operators to spinless fermion operators [48–50]:

$$\sigma_j^z = 1 - 2c_j^{\dagger}c_j,$$

$$\sigma_j^x = e^{i\phi_j}(c_j^{\dagger} + c_j),$$

$$\sigma_j^y = ie^{i\phi_j}(c_j^{\dagger} - c_j),$$
(5)

with  $\phi_j$  being the phase string generated by all earlier sites along the chain,  $\phi_j = \pi \sum_{l < j} c_l^{\dagger} c_l$ . Neglecting

boundary terms we arrive at a simple bilinear form of the Hamiltonian expressed by spinless fermions:

$$\mathcal{H} = \sum_{j} \left[ J_{o} \left( e^{i\theta} c_{2j-1}^{\dagger} c_{2j}^{\dagger} + c_{2j-1}^{\dagger} c_{2j} \right) + J_{e} \left( e^{-i\theta} c_{2j}^{\dagger} c_{2j+1}^{\dagger} \right) + c_{2j}^{\dagger} c_{2j+1} \right] + c_{2j}^{\dagger} c_{2j+1} + c_{2j}^{\dagger} c_{2j+1} + c_{2j}^{\dagger} c_{2j+2} + \text{H.c.} \right]. (6)$$

The fermionized version of the model (6) corresponds to a p-wave superconductor in which the electrons have next nearest neighbor hopping. There is a relative phase  $e^{i\theta}$  between the nearest neighbor hopping and the nearest neighbor pairing. The present model is also dual to an extended Su-Schrieffer-Heeger (SSH) model [51, 52].

# C. Majorana zero modes of topological nontrivial states

In this Section we explore the zero modes via the Bogoliubov-de Gennes (BdG) equations with open boundary condition (OBC). Generally, Hamiltonian (6) is not PT symmetric except for  $\theta = \pi/2$  when the p-wave pairing amplitude is purely imaginary. It can be diagonalized with a linear transformation of the canonical fermion operators  $\{c, c^{\dagger}\}$ ,

$$\mathcal{H} = \sum_{i,j} \left[ c_i^{\dagger} A_{ij} c_j + \frac{1}{2} \left( c_i^{\dagger} B_{ij} c_j^{\dagger} - c_i B_{ij}^* c_j \right) \right], \quad (7)$$

with

$$A_{ij} = J_i(\delta_{i,j-1} + \delta_{i,j+1}) + 2K(\delta_{i,j-2} + \delta_{i,j+2}),$$
  

$$B_{ij} = \Delta_i(\delta_{i,j-1} - \delta_{i,j+1}),$$
(8)

where  $J_i = J_o (J_e)$  and  $\Delta_i \equiv J_o e^{i\theta} (\Delta_i \equiv J_e e^{-i\theta})$  when  $i \in \text{odd}$  (even). A(B) is a  $N \times N$  symmetric (antisymmetric) matrix. Hamiltonian (6) can be diagonalized by using the BdG transformation:

$$\eta_n^{\dagger} = \sum_{i=1}^{N} \left( u_{n,i} c_i^{\dagger} + v_{n,i}^* c_i \right),$$
(9)

where n and i are indices of eigenvalues and lattice sites, respectively. The spectra  $\Lambda_n$  and eigenvectors  $u_{n,i}$  and  $v_{n,i}$  can be determined by solving BdG equations [54]:

$$\begin{pmatrix} A & B \\ -B^* & -A^T \end{pmatrix} \begin{pmatrix} u_{n,i} \\ v_{n,i}^* \end{pmatrix} = \Lambda_n \begin{pmatrix} u_{n,i} \\ v_{n,i}^* \end{pmatrix}. \tag{10}$$

The BdG Hamiltonian satisfies an imposed symmetry, i.e., particle-hole symmetry (PHS), in the form  $\tau^x \mathcal{H}^T \tau^x = -\mathcal{H}$ , where the Pauli matrix  $\tau^x$  acts in Nambu space. Hence the energy levels must come in  $\pm \Lambda$  conjugate pairs except the zero energy mode which is self-conjugate. The topological point defects in the 1D model trap zero-energy bound states and induce at most one protected zero-energy mode localized at each end of an

open chain. The existence of a zero-energy localized states can be interpreted as a signature of Majorana modes.

Figure 2 shows the energy spectrum for the GCM with OBC for two characteristic angles  $\theta$ . At  $\theta = \pi/3$  which is isomorphic with  $e_g$  orbital model [53] there exist zero modes for  $|K| \leq 1$  shown in Fig. 2(a). Extensive data reveals that such edge modes are protected by energy gaps away from critical points. The model for  $\theta \neq \pi/2$  can be modified continuously to a Kitaev model in the topological nontrivial phase without closing the band gap, so the model in such a phase was featured by the presence of zero-energy Majorana edge states under the OBC, namely,  $n_M = 1$ . According to Eq. (6), topological phase transitions of the model are classified in terms of the number of isolated Majorana zero modes  $n_M$ . These Majorana states are stable against quadratic perturbations which preserve the symmetries.

In contrast, there is no zero mode at  $\theta = \pi/2$  irrespective of K, see Fig. 2(b). We note that at K=0 there is a macroscopic number  $2^{N/2-1}$  of states condensed at zero-energy modes [2, 55] but they are not edge modes. The three-site interactions remove the macroscopic degeneracy instantly and zero-energy states become dispersive. Interestingly, the tower of these low-energy excitations keep intact as K increases, and they are separated from higher energy states by a linear dispersion.

## D. Pfaffian $\mathbb{Z}_2$ invariant for BdG Hamiltonian and topological phase transition

Next discrete Fourier transformation for plural spin sites is introduced for the periodic boundary conditions,

$$c_{2j-1} = \frac{1}{\sqrt{N'}} \sum_{k} e^{-ikj} a_k, \quad c_{2j} = \frac{1}{\sqrt{N'}} \sum_{k} e^{-ikj} b_k, (11)$$

with the discrete momenta as

$$k = \frac{n\pi}{N'}, \quad n = -(N'-1), -(N'-3), \dots, (N'-1).(12)$$

Then we write the Hamiltonian in the BdG form in terms of Nambu spinors,

$$\mathcal{H} = \sum_{k} \Gamma_{k}^{\dagger} \hat{M}_{k} \Gamma_{k}, \tag{13}$$

where

$$\hat{M}_{k} = \frac{1}{2} \begin{pmatrix} F_{k} & S_{k} & 0 & T_{k} \\ S_{k}^{*} & F_{k} & -T_{-k} & 0 \\ 0 & -T_{-k}^{*} & -F_{k} & -S_{-k}^{*} \\ T_{k}^{*} & 0 & -S_{-k} & -F_{k} \end{pmatrix}, \quad (14)$$

and  $\Gamma_k^\dagger=(a_k^\dagger,b_k^\dagger,a_{-k},b_{-k})$  . The matrix elements in Eq. (14) are:

$$T_k = J_o e^{i\theta} - J_e e^{i(k-\theta)},$$
  

$$S_k = J_o + J_e e^{ik},$$
  

$$F_k = 2K \cos k.$$
 (15)

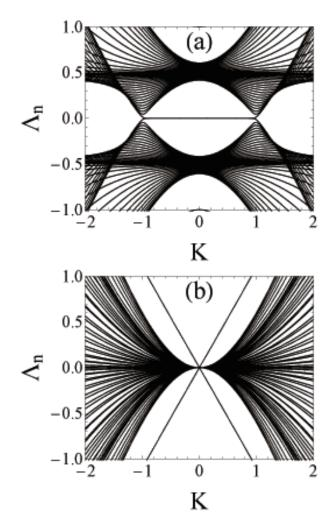


FIG. 2: Energy spectrum for the GCM with the OBC for N=80 sites. The orbital angle  $\theta$  is: (a)  $\theta=\pi/3$ ; (b)  $\theta=\pi/2$ . Parameters are as follows:  $J_o=1,\ J_e=4$ .

The system belongs to topological class D with a topological invariant  $\mathbb{Z}_2$  in one dimension [56], which satisfies

$$C^{-1}\hat{M}(-k)C = -\hat{M}(k). \tag{16}$$

Here  $C = \tau^x \otimes \sigma^0 \mathcal{K}$ , where  $\tau^x$  and  $\sigma^0$  are the Pauli matrices acting on particle-hole space and spin space, respectively, and  $\mathcal{K}$  is the complex conjugate operator.

Following the basic definition of particle-hole  $\mathcal{C}$ , an auxiliary function  $W(k) = \hat{M}_{4\times 4}(k)\mathcal{C}$  is defined, and we have  $W(k)^T = -W(-k)$ . For particle-hole symmetric momenta  $k \in \{0, \pm \pi\}$  in Brillouin zone, we have  $W(0)^T = -W(0)$  and  $W(\pi)^T = -W(\pi)$ , which are both skew matrices. The topology of the GCM can be characterized by the Pfaffian of the Hamiltonian at k=0 and  $\pi$ , with  $\nu = sgn\{Pf(W(0))Pf(W(\pi))\}$ . Here  $\nu$  is a topological protected number, which means that  $\nu$  will never change sign upon deformation as long as the energy gap at k=0 and  $\pi$  is not closed. Then  $\nu=-1$  (+1) corresponds to the topological nontrivial (trivial)

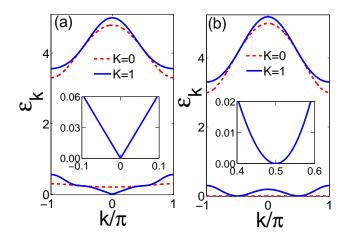


FIG. 3: Dispersion relations (19) for the GCM for three selected values of three-spin interactions K=0 and 1 at: (a)  $\theta=\pi/3$  and (b)  $\theta=\pi/2$ . Insets show amplifications of lower energies  $\varepsilon_{k,1}$  near Fermi surface at K=1. Parameters are as follows:  $J_o=1$ ,  $J_e=4$ .

phase, respectively [57, 58]. The Pfaffian reads

$$Pf[W(0)] = 4J_oJ_e\cos^2\theta - 4K^2,$$
  
 $Pf[W(\pi)] = -4J_oJ_e\cos^2\theta - 4K^2.$  (17)

It is easy to find that in the regions  $|K| \leq \sqrt{J_o J_e} \cos \theta$ , a topological nontrivial phase with  $\nu = (-1)^{n_M}$  is accompanied with a zero-energy Majorana mode in Fig. 2.

### III. QUANTUM PHASE TRANSITION

Along these lines, we obtain the diagonal form of the Hamiltonian Eq. (14),

$$\mathcal{H} = \sum_{k} \sum_{j=1}^{2} \varepsilon_{k,j} \left( \gamma_{k,j}^{\dagger} \gamma_{k,j} - \frac{1}{2} \right). \tag{18}$$

The spectra consist of two branches of energies  $\varepsilon_{k,j} > 0$  (j=1,2), given by the following expressions:

$$\varepsilon_{k,1(2)} = \sqrt{\varsigma_k \pm \sqrt{\tau_k}},$$
 (19)

where

$$\varsigma_{k} = \frac{1}{2}(|T_{k}|^{2} + |T_{-k}|^{2}) + |S_{k}|^{2} + F_{k}^{2},$$

$$\tau_{k} = \frac{1}{4}(|T_{k}|^{2} - |T_{-k}|^{2})^{2} + |S_{k}^{*}T_{k} + S_{k}T_{-k}|^{2}$$

$$+ 4|S_{k}|^{2}F_{k}^{2}.$$
(20)

Note that  $\tau_k$  is always positive for any momentum k. We remark that the energy spectrum  $\varepsilon_{k,j}$  (j=1,2) is thus always positive which is different from the compass spin chain with the (XZY-YZX)-type of three-site interaction [37]. The form of  $F_k$  (15) leads to a crossing of excitations at  $k=\pm\pi/2$  for diverse values of K, see Fig. 3.

The most important properties of the 1D spin system are manifested in the ground state. The ground-state energy density of our model can be written as

$$e_0 = -\frac{1}{2N} \sum_{k} (\varepsilon_{k,1} + \varepsilon_{k,2})$$
$$= -\frac{1}{\sqrt{2N}} \sum_{k} \sqrt{\varsigma_k + \sqrt{\varsigma_k^2 - \tau_k}}.$$
 (22)

From Eq. (6), K promotes the hopping between next nearest neighbor sites and modifies the corresponding dispersions. The phase diagram of the GCM under three-site interactions can be analytically calculated by investigating the gap closing of the spectrum (19). Accordingly, the spectral gap is determined by the first energy branch, i.e.,  $\Delta = 2 \min_k \{\varepsilon_{k,1}\}$ . The gap closes at some critical momentum  $k_c$  delimited by  $\varsigma_{k_c}^2 = \tau_{k_c}$ . One finds that this condition can be satisfied only when

$$\cos k_c = 1$$
 and  $K_c = \pm \sqrt{J_o J_e} \cos \theta$ . (23)

When the magnitude |K| of three-site interactions (6) is below the critical field,  $K_c = \sqrt{J_o J_e} \cos \theta$  [see Fig. 3(a)], the ground state is a canted antiferromagnetic phase dominated by nearest neighbor correlation functions along the x axis [35]. On the contrary, the system becomes a spin-spiral phase for  $|K| > K_c$ . Unlike Ising model with XZX-type interactions where the gap-closing momentum  $k_c$  moves in the Brillouin zone along the critical lines [30], in our case  $k_c$  is suited at Brillouin zone center  $k_c = 0$  constrained by the P symmetry.

It is clear that the critical lines  $K = -\sqrt{J_oJ_e}\cos\theta$  and  $K = \sqrt{J_oJ_e}\cos\theta$  will get closer as  $\theta$  approaches  $\pi/2$ . At  $\theta = \pi/2$ , the 1D GCM Eq. (4) describes a competition between two pseudospin components,  $\{\sigma_i^x, \sigma_i^y\}$ , and has the highest possible frustration of interactions. The mixed terms  $\propto \sigma_i^x \sigma_{i+1}^y$  can be eliminated by writing this model in the form of the GCM with rotated pseudospin components, where the rotation by angle  $\theta = \pi/4$  anticlockwise with respect to the z axis in the pseudospin space is made, i.e.,  $\bar{\sigma}_i^x \equiv (\sigma_i^x + \sigma_i^y)/\sqrt{2}$ ,  $\bar{\sigma}_i^y \equiv (\sigma_i^y - \sigma_i^x)/\sqrt{2}$ , and one finds

$$\bar{\mathcal{H}} = \sum_{i=1}^{N'} \left( J_o \bar{\sigma}_{2i-1}^x \bar{\sigma}_{2i}^x + J_e \bar{\sigma}_{2i}^y \bar{\sigma}_{2i+1}^y \right) + \sum_{i=1}^{N} K(\bar{\sigma}_{i-1}^x \sigma_i^z \bar{\sigma}_{i+1}^x + \bar{\sigma}_{i-1}^y \sigma_i^z \bar{\sigma}_{i+1}^y ). \tag{24}$$

By performing a similar analytical process as Eq. (13), we can diagonalize the rotated Hamiltonian in the form of

$$\bar{\mathcal{H}} = \sum_{k} \bar{\Gamma}_{k}^{\dagger} \hat{\bar{M}}_{k} \bar{\Gamma}_{k}, \qquad (25)$$

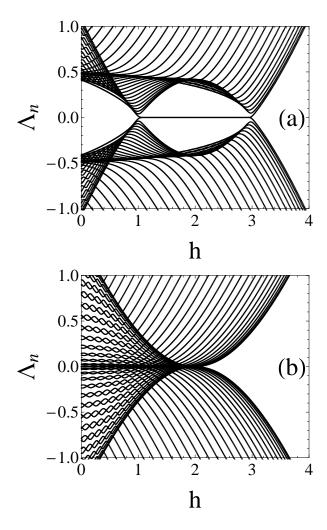


FIG. 4: Energy spectrum for the GCM with parameters: (a)  $\theta = \pi/3$ , and (b)  $\theta = \pi/2$  under the OBC. Parameters are as follows:  $J_o = 1$ ,  $J_e = 4$ , K = 2 and N = 80.

where

$$\hat{\bar{M}}_{k} = \frac{1}{2} \begin{pmatrix} \bar{F}_{k} & \bar{S}_{k} & 0 & \bar{T}_{k} \\ \bar{S}_{k}^{*} & \bar{F}_{k} & -\bar{T}_{-k} & 0 \\ 0 & -\bar{T}_{-k}^{*} & -\bar{F}_{k} & -\bar{S}_{k} \\ \bar{T}_{k}^{*} & 0 & -\bar{S}_{k}^{*} & -\bar{F}_{k} \end{pmatrix},$$
(26)

with

$$\bar{T}_k = J_o + J_e e^{ik}, 
\bar{S}_k = J_o + J_e e^{ik}, 
\bar{F}_k = 2K \cos k,$$
(27)

and  $\bar{\Gamma}_k^{\dagger} = (\bar{a}_k^{\dagger}, \bar{b}_k^{\dagger}, \bar{a}_{-k}, \bar{b}_{-k})$ . Then we have

$$\varepsilon_{k,1(2)} = \sqrt{|\bar{T}_k|^2 + |\bar{F}_k|^2} \pm |\bar{T}_k|.$$
 (28)

It is evident that there is a zero-energy flat band for K=0 which is susceptible to residual interactions. We note that  $\bar{F}_k$  (27) is vanishing at commensurate momenta  $k=\pm\pi/2$ . Therefore, the system turns to be gapless, as recognized in Fig. 3(b).

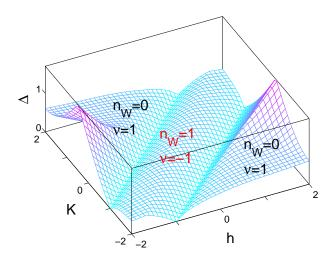


FIG. 5: The excitation gap  $\Delta$  as functions of three-site interactions  $\propto K$  and magnetic field h. Here  $n_W$  denotes the number of Majorana zero modes and  $\nu$  characterize the Pfaffian topological invariant. Parameters are as follows:  $J_o = 1$ ,  $J_e = 4$ ,  $\theta = \pi/3$ .

### IV. GENERALIZED COMPASS MODEL IN A HOMOGENOUS MAGNETIC FIELD

Here we study the effect of a homogenous magnetic field. We consider the case where the magnetic field is oriented perpendicular to the easy plane of the spins, i.e.,  $\vec{h}_o = \vec{h}_e = h\hat{z}$ . h is the magnitude of the transverse external field, which contains the g-factor g and the Bohr magneton  $\mu_{\rm B}$ .

The magnetic field does not spoil the zero-energy edge states at  $\theta = \pi/3$ , as shown in Fig. 4(a). The inclusion of homogenous magnetic fields replaces  $F_k$  in Eq. (14) with  $F_k \to F_k' = 2K\cos k - 2h$ . The gap as a function of K and h is shown in Fig. 5. The critical lines are pinpointed at  $K - h = \pm 1$  for  $J_o = 1$ ,  $J_e = 4$ ,  $\theta = \pi/3$ , as depicted in Fig. 5. It is easy to see that the critical lines found at  $h = \pm 1$  in the absence of K are moved to  $K - h = \pm 1$  when the additional (XZX+YZY)-type interaction emerges. In the phase diagram of Fig. 5 at least three phases can be specified: two z-axis polarized phases for positive (negative) h, and a canted Néel (CN) phase for moderate h. Such QPTs are of second order since the second derivative of the ground-state energy density  $e_0$  exhibits divergence, as shown in Fig. 6.

In the limit of large h, the system stays in a polarized state with  $\langle \sigma_i^x \sigma_{i+1}^x \rangle \to 0$ ,  $\langle \sigma_i^y \sigma_{i+1}^y \rangle \to 0$ , and  $\langle \sigma_i^z \sigma_{i+1}^z \rangle \to 1$ . In contrast, in the limit of large K all the nearest neighbor spin correlations vanish, corresponding to a spiral spin state. According to the phase diagram of Ising model with (XZX+YZY) interactions given in Ref. [20], the existence of an additional phase IV was suggested. However, such a phase is not confirmed in our investigation, and we believe that a crossover from the

spin-spiral state to the spin-polarized state takes place instead.

The critical behavior is determined by those lowenergy states near the critical mode  $(k \sim k_c)$ . As happroaches  $h_c$ , the gap vanishes as  $\Delta \sim (h - h_c)^{\nu_h z}$ , where  $\nu_h$  and z are the correlation length and dynamic exponents, respectively. The gap near criticality is

$$\Delta \simeq \frac{4\sqrt{J_o J_e} \cos \theta}{J_o + J_o} |h - h_c|, \tag{29}$$

and one finds the critical exponent  $\nu_h z = 1$ . Since the size dependence of the gap,  $\Delta \sim L^{-z}$ , defines the dynamic exponent z, we expand the gap around the critical line  $h_c$  from threshold critical mode  $k_c$ , i.e., at  $|k - k_c| \ll 1$ ,

$$\varepsilon_k \sim \frac{\sqrt{\varsigma_k^2 - \tau_k}}{\sqrt{2\varsigma_k}} \sim \frac{2J_o J_e \cos^2 \theta}{J_o + J_e} |k|.$$
 (30)

The dynamic critical exponent z relates the scaling of energy (or time) scales to length scales. The relativistic spectra at  $k_c$  imply a dynamical exponent z=1 [for  $\theta \neq \pi/2$  in inset of Fig. 3(a)] and the Fermi velocity is independent of h and K. The correlation-length exponent  $\nu_h=1$  here confirms that 1D GCM belongs to the same universality as the 1D Ising model under the transverse field.

For  $\theta=\pi/2$ , a finite magnetic field will modify the energy spectra through  $\bar{F}_k \to \bar{F}_k' = 2K\cos k - 2h$  in Eq. (26), as is uncovered in Fig. 7(a). To this end,  $\bar{F}_k'$  can be zero when  $|h/K| \leq 1$ , and this causes a closure of the gap at an incommensurate momentum  $k_c = \arccos(h/K)$ . Therefore, the system remains gapless as long as  $|h/K| \leq 1$ , as evidenced in Fig. 7(b). There is no spontaneous symmetry breaking in this spinliquid phase across the quantum critical point (QCP),

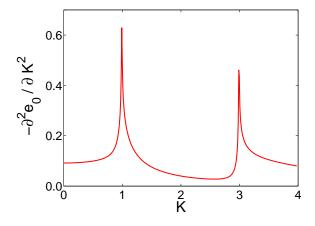


FIG. 6: The second derivative of the ground-state energy density,  $-(\partial^2 e_0/\partial K^2)$ , for h=2. Parameters are as follows:  $J_o=1,\ J_e=4,\ \theta=\pi/3$ .

since the ground-state energy density,

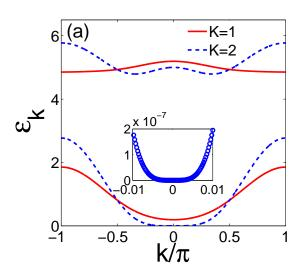
$$e_0 = -\frac{1}{N} \sum_k \sqrt{J_o^2 + J_e^2 + 2J_o J_e \cos k + 4(K \cos k - h)^2},$$

(31)

is infinitely differentiable during this transition. The phase transition is a Berezinskii-Kosterlitz-Thouless (BKT) transition. In the spin-liquid phase, one can find the spectra vanish at  $k_c$ ,

$$\varepsilon_k \sim \frac{2(K^2 - h^2)}{\sqrt{J_o^2 + J_e^2 + 2J_oJ_eh/K}} (k - k_c)^2.$$
(32)

Such quadratic dispersion (32) corresponds to a dynamical exponent z=2 [see inset of Fig. 3(b)]. While expanding the gap around the QCP from upper threshold one finds the excitations follow a power-law dependence



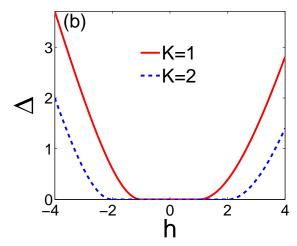


FIG. 7: (a) The dispersion relations for different K with h=2; (b) The excitation gap  $\Delta$  as functions of h for different K=1,2. Inset in (a) shows the amplification of lower energies  $\varepsilon_{k,1}$  near Fermi surface at K=2. Parameters are as follows:  $J_o=1,\ J_e=4,\ \theta=\pi/2$ .

on k,

$$\varepsilon_k \sim \frac{h^2}{2(J_o + J_e)} \, k^4. \tag{33}$$

We confirm the dispersion of fermions is described by a biquadratic parabola [see inset of Fig. 7(b)], and the momentum dependence of the charge excitations suggests a large dynamical exponent z=4. This leads to a higher density of states above the gap  $D(\varepsilon)\sim \varepsilon^{-3/4}$  than for the standard 1D van Hove singularity with  $D(\varepsilon)\sim \varepsilon^{-1/2}$  (here  $\varepsilon$  is the energy measured from the band edge). Those low-energy states in the gapless regime near the critical modes determine the critical behavior. Both the low-temperature entropy  $\mathcal S$  and the specific heat  $C_V$  present a power-law dependence on temperature as  $T^{d/z}$  (here the spatial dimension d is 1), which can be readily measured in experiments [59–61]. Meanwhile, the gap near criticality is

$$\Delta \simeq \frac{2}{J_0 + J_e} |h - h_c|^2, \tag{34}$$

and one finds the critical exponent  $\nu_h z = 2$ . The outcome  $\nu_h = 1/2$  for the 1D compass model is different from other points [62, 63] obtained from scaling of fidelity susceptibility, which is discussed in Sec. V A. The unusual behavior which takes place due to the multicriticality of such QPTs has been recognized [64]. Such anomalous feature, such as a flat dispersion like  $k^4$  resembles QPTs between the Mott insulator and metal in 2D square lattice by controlling the filling [65]. Such a new universality class may be characterized by an emergent super-symmetry at a multicritical point [66].

## V. QUANTUM INFORMATION THEORETICAL MEASURES

Interdisciplinary studies have harvested rich but rather mixed research findings in the past decades. A blooming topic is the characterization of QPTs in terms of the ideas from the field of quantum information in recent years. Different from traditional descriptions of phase transitions in the theory of condensed matter, the local order parameters, key ingredients of Ginzburg-Landau-Wilson paradigm, are not necessary in such a formalism. Instead, quantum information approaches tend to capture the nonlocal information and universal properties near criticality despite the great diversity of the nature of miscellaneous phases.

It should be emphasized that the entanglement entropy [67, 68] and the fidelity susceptibility are frequently considered. As a new perspective of the phase transitions and the associated universality, they have proven to be useful measures. In this respect, when a quantum system moves across a QPT separating two fundamentally different ground states by varying external control parameters, physical observables often exhibit singular behavior

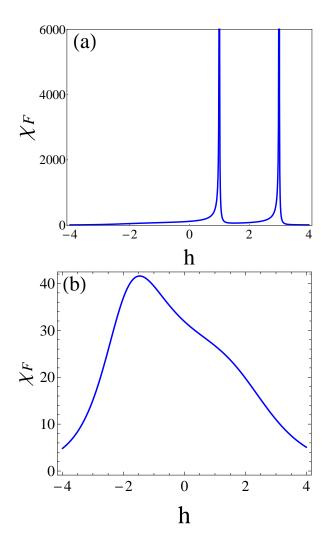


FIG. 8: The fidelity as a function of h for the GCM with three-site interactions (4) for: (a)  $\theta = \pi/3$  and (b)  $\pi/2$ . Parameters:  $J_o = 1$ ,  $J_e = 4$ , K = 2, N = 1000.

which is ascribed to the gapless excitation and divergence of correlation length at the QCPs. Frequently this picture can be visualized when there are symmetry breaking states on either side or both sides of a QPT. However, a topological phase transition follows from a change of topological index of the ground state and the topological phase of matter is not related to the spontaneous symmetry breaking. Therefore, a local order parameter has no scope for its ability to sense the topological QPT.

#### A. Fidelity susceptibility

The fidelity susceptibility is a general probe of phase transition which originates from Anderson's orthogonality catastrophe. By definition, quantum fidelity of a many-body Hamiltonian  $\hat{H}(\lambda) = H_0 + \lambda H_I$  is [69]

$$F(\lambda_0, \lambda_1) = |\langle \Psi_0(\lambda_0) | \Psi_0(\lambda_1) \rangle|, \tag{35}$$

where  $|\Psi_0\rangle$  is the ground state,  $\lambda_0$  and  $\lambda_1$  specify two points in the parameter space of driving parameter  $\lambda$ . In this respect, fidelity susceptibility is defined as first nonzero order of the Taylor expansion of the overlap function  $F(\lambda, \lambda + \delta\lambda)$ , given by [70, 71]

$$\chi_F = \lim_{\delta \lambda \to 0} \frac{-2 \ln F(\lambda, \lambda + \delta \lambda)}{(\delta \lambda)^2}.$$
 (36)

The concept of quantum fidelity susceptibility has been recognized as a versatile indicator in identifying QCPs and universality class by the finite-size scaling behavior [72]. Interestingly, a holographic description for the fidelity susceptibility in conformal field theories is a volume of maximal time slice in an anti-de Sitter space-time when the perturbation is exactly marginal [73]. However, the application of the fidelity susceptibility to detect a BKT transition is controversial: On the one hand, some investigations are in favor that the fidelity susceptibility is able to discriminate the critical lines of BKT transitions with a logarithmic divergence [74, 75], while on the other hand, some disprove it [76, 77]. This shows that indeed an in-depth understanding of the underlying physics is still missing.

We add to this discussion and present the fidelity susceptibility for  $\theta = \pi/3$  and  $\theta = \pi/2$  with K = 1; more details of the calculation can be found in Appendix A. The fidelity susceptibility for  $\theta = \pi/3$  detects the second-order QPTs, seen Fig. 8(a), while such a transition is absent for  $\theta = \pi/2$  shown in Fig. 8(b). Our findings suggest that the fidelity susceptibility does not diverge at BKT-type QPTs in one spatial dimension.

#### B. Coherence susceptibility

In the representation spanned by the two-qubit product states we employ the following basis,

$$\{|0\rangle_i \otimes |0\rangle_j, |0\rangle_i \otimes |1\rangle_j, |1\rangle_i \otimes |0\rangle_j, |1\rangle_i \otimes |1\rangle_j\},$$
 (37)

where  $|0\rangle$  ( $|1\rangle$ ) denotes spin up (down) state, the two-site density matrix can be expressed as,

$$\rho_{ij} = \frac{1}{4} \sum_{a,a'=0}^{3} \langle \sigma_i^a \sigma_j^{a'} \rangle \sigma_i^a \sigma_j^{a'}, \tag{38}$$

where  $\sigma_i^a$  are Pauli matrices  $\sigma_i^x$ ,  $\sigma_i^y$ , and  $\sigma_i^z$  for a=1,2,3, and a  $2\times 2$  unit matrix for a=0. The Hamiltonian has  $\mathbb{Z}_2$  symmetry, namely, the invariance under parity transformation  $P=\otimes_i\sigma_i^z$ , and then correlation functions such as  $\langle \sigma_i^a\sigma_j^b \rangle$  (a=x,y and b=0,z) vanish simultaneously. Usually people believe that  $\langle \sigma_i^x\sigma_j^y \rangle$  ( $\langle \sigma_i^y\sigma_j^x \rangle$ ) vanishes due to the imaginary character of  $\sigma_j^y$  ( $\sigma_i^y$ ). Here we disprove this argument in our model due to its complex nature of Hamiltonian (4) in Appendix B. Also, be aware that the relations between correlations where

$$\langle \sigma_0^z \sigma_r^z \rangle = \langle \sigma_0^z \rangle \langle \sigma_r^z \rangle - G_r G_{-r} \tag{39}$$

is not always valid for a complex Hamiltonian [see the definition of  $G_r$  in Eq.(B3)]. A number of results have been focused on translation-invariant systems and almost exclusively correspond to reflection-symmetric systems, despite the fact that models violating reflection invariance play a prominent role in many-body theory, e.g., in describing interactions of DM interactions or three-site (XZY-YZX)-type interactions [78].

Therefore, the two-qubit density matrix reduces to an X-state,

$$\rho_{ij} = \begin{pmatrix} u^+ & 0 & 0 & z_1 \\ 0 & w_1 & z_2 & 0 \\ 0 & z_2^* & w_2 & 0 \\ z_1^* & 0 & 0 & u^- \end{pmatrix},$$
(40)

with

$$u^{\pm} = \frac{1}{4} (1 \pm 2 \langle \sigma_i^z \rangle + \langle \sigma_i^z \sigma_j^z \rangle), \tag{41}$$

$$z_1 = \frac{1}{4} (\langle \sigma_i^x \sigma_j^x \rangle - \langle \sigma_i^y \sigma_j^y \rangle - i \langle \sigma_i^x \sigma_j^y \rangle - i \langle \sigma_i^y \sigma_j^x \rangle), \tag{42}$$

$$z_2 = \frac{1}{4} (\langle \sigma_i^x \sigma_j^x \rangle + \langle \sigma_i^y \sigma_j^y \rangle + i \langle \sigma_i^x \sigma_j^y \rangle - i \langle \sigma_i^y \sigma_j^x \rangle), \tag{43}$$

$$\omega_1 = \omega_2 = \frac{1}{4} (1 - \langle \sigma_i^z \sigma_j^z \rangle). \tag{44}$$

The density matrix of a single qubit is easily obtained by a partial trace over one of the two qubits,

$$\rho_i = \begin{pmatrix} \frac{1}{2} (1 + \langle \sigma_i^z \rangle) & 0\\ 0 & \frac{1}{2} (1 - \langle \sigma_i^z \rangle) \end{pmatrix}. \tag{45}$$

One easily finds that

$$S(\rho_i) = S(\rho_j) = -\sum_{m=0}^{1} \{ [1 + (-1)^m \langle \sigma_i^z \rangle] / 2 \}$$

$$\times \log_2 \{ [1 + (-1)^m \langle \sigma_i^z \rangle] / 2 \}, \tag{46}$$

and

$$S(\rho_{ij}) = -\sum_{m=0}^{1} \xi_m \log_2 \xi_m - \sum_{n=0}^{1} \xi_n \log_2 \xi_n,$$
 (47)

where

$$\xi_m = \frac{1}{4} \left[ 1 + \langle \sigma_i^z \sigma_j^z \rangle + (-1)^m \sqrt{(\langle \sigma_i^x \sigma_j^x \rangle - \langle \sigma_i^y \sigma_j^y \rangle)^2 + (\langle \sigma_i^x \sigma_j^y \rangle + \langle \sigma_i^y \sigma_j^x \rangle)^2 + 4\langle \sigma_i^z \rangle^2} \right], \tag{48}$$

$$\xi_n = \frac{1}{4} \left[ 1 - \langle \sigma_i^z \sigma_j^z \rangle + (-1)^n \sqrt{(\langle \sigma_i^x \sigma_j^x \rangle + \langle \sigma_i^y \sigma_j^y \rangle)^2 + (\langle \sigma_i^x \sigma_j^y \rangle - \langle \sigma_i^y \sigma_j^x \rangle)^2} \right]. \tag{49}$$

A simplified form of relative entropy has been proven

as a valid measure of coherence for a given basis:

$$C(\rho_{ij}) = S(\rho_{diag}) - S(\rho_{ij}), \tag{50}$$

where  $S(\bullet)$  stands for the von Neumann entropy of  $\bullet$  and  $\rho_{diag}$  is obtained from  $\rho$  by removing all its off-diagonal entries. The non-analyticity of the ground state at QCPs can be characterized by the singularity of the coherence susceptibility [79], which is defined as

$$\chi^{co} \equiv \partial C(\rho)/\partial \lambda. \tag{51}$$

Here,  $\rho$  stands either for the density operator of the whole system or for the reduced density operator of a subsystem.

It was interesting to note that quantum discord, in contrast to entanglement, is able to signal the BKT-type QPTs [80–82]. The quantum discord was introduced to quantify non-classical correlations beyond entanglement paradigm in quantum states and thus was given by the difference of the mutual information  $I(\rho)$  and the classical correlation  $J(\rho)$  [83],

$$D(\rho) = I(\rho) - J(\rho). \tag{52}$$

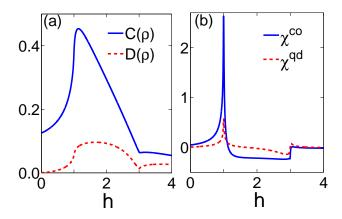


FIG. 9: Characterization of the ground state for the model Eq. (4) at  $\theta=\pi/3$  for increasing magnetic field h: (a) relative entropy  $C(\rho)$  and quantum discord  $D(\rho)$ , and (b) coherence susceptibility  $\chi^{co}$  and discord susceptibility  $\chi^{qd}$ . Other parameters:  $J_o=1,\ J_e=4,\ K=2$  for N=200.

Similarly we can define discord susceptibility,

$$\chi^{qd} \equiv \partial D(\rho)/\partial \lambda. \tag{53}$$

The relative entropy and quantum discord as functions of h at K=2 are plotted in Fig. 9. We find that both quantities share similar trends and there are sharp changes across the QPTs. The peaks of their susceptibilities at h=1 and the step-like behavior at h=3 indicate the QCPs.

We emphasize that quantum correlations for  $\theta = \pi/2$  revealed by the relative entropy and the quantum discord exhibit distinct behavior from the case with  $\theta = \pi/3$ , as seen in Fig. 10. Both quantities show their local maxima close to  $h = \pm K$ . However, we find that these indictors behave in a more distinct way in the regime of large K. For small K two local maxima affect each other and move the positions of maxima from the true QCPs. In addition, we find that concurrence, another measure of entanglement [84], and von Neumann entropy display similar behaviors with fidelity susceptibility (not shown).

### VI. CONCLUSION

In the paper we analyze quantum phase transitions in a class of the one-dimensional compass models with an (XZX+YZY)-type of three-site interactions. We present the exact solution by means of Jordan-Wigner transformation, and study the fermionic spectra, excitation gap, critical exponents, and established the phase diagram. For general titling angle  $\theta$ , the three-site (XZX+YZY) interactions renormalize the effect of magnetic field and thus a nontrivial magnetoelectric effect can be expected. In the canted Néel phase (weak-coupling BCS regime in spinless fermions), it exhibits a pair of zero-energy Majorana modes at each end of the open chain, and it is also characterized with a Pfaffian topological invariant  $\nu = -1$  with periodic boundary condition.

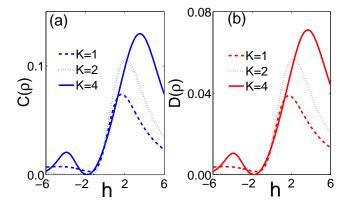


FIG. 10: Characterization of the ground state for the model Eq. (4) at  $\theta = \pi/2$  for increasing magnetic field h and for selected values of K: (a) relative entropy  $C(\rho)$  and (b) quantum discord  $D(\rho)$ . Other parameters:  $J_o = 1$  and  $J_e = 4$  for N = 200.

In the compass limit the competition between the three-site (XZX+YZY) interactions and the magnetic field drives the system into a gapless phase through a Berezinskii-Kosterlitz-Thouless transition. The dynamic exponent is a measure for characterizing the coherence of the system and it is found to be z=4 across the quantum critical points. Thus, coherence is very sensitive to whether the system is at the compass limit, i.e., at the angle  $\theta=\pi/2$  which is more incoherent than the other cases. It has been shown that z can be extracted from the measurement of the low-temperature specific heat and entropy in the Tomonaga-Luttinger-liquid phase.

To complete the analytic approach, we present a study of diverse measures of quantum correlations including fidelity susceptibility, von Neumann entropy, relative entropy, coherence susceptibility, pairwise concurrence and quantum discord in the generalized compass chain with three-site (XZX+YZY) interactions. Analytical expressions are obtained from the spin-spin correlation functions. We show that all these measures can be useful to detect the second-order transition, while only the relative entropy and the quantum discord can signal the Berezinskii-Kosterlitz-Thouless transition. We note that the one-dimensional compass model with (XZX+YZY)type interactions can provide an ideal benchmark for other computational methods to testify the Berezinskii-Kosterlitz-Thouless quantum phase transition. We also point out that deriving the correlation functions for the systems with broken reflection symmetry requires a rather careful and subtle procedure.

#### Acknowledgments

We thank G.-S. Tian, Dazhi Xu, Yunfeng Cai, Y.-L. Dong and Hua Jiang for insightful discussions. This work was supported by the Natural Science Foundation of Jiangsu Province of China under Grant No. BK20141190 and the NSFC under Grant Nos. 11474211, 11504253, 21473240. A. M. O. kindly acknowledges support by Narodowe Centrum Nauki (NCN, National Science Center) under Project No. 2012/04/A/ST3/00331.

# Appendix A: Eigenstates and eigenvalues of generalized compass model

By Fourier transforming the GCM Hamiltonian (14) and grouping together terms with k and -k, H is transformed into a sum of commuting Hamiltonians  $H_k$  describing a different k mode each. Then we can obtain the spectrum of the GCM by diagonalizing each Hamiltonian mode  $H_k$  independently.

Formally we write the Hamiltonian mode  $H_k$  in the BdG form,

$$\hat{H}_k = \Gamma_k^{\dagger} \hat{M}_k \Gamma_k, \tag{A1}$$

and  $\Gamma_k^\dagger \equiv (a_k^\dagger,a_{-k},b_k^\dagger,b_{-k}).$   $\hat{M}_k$  can be diagonalized by a unitary transformation,

$$\hat{H}_{k} = \Gamma_{k}^{\dagger} U_{k} U_{K}^{\dagger} M_{k}^{\prime} U_{K} U_{k}^{\dagger} \Gamma_{k}$$

$$= \sum_{k} \Gamma_{k}^{\prime \dagger} D_{k} \Gamma_{k}^{\prime}, \qquad (A2)$$

where  $\Gamma_k'\!=\!U_k^\dagger\Gamma_k,$  i.e., the diagonalized form is achieved by a four-dimensional Bogoliubov transformation which connects the original operators  $\{a_k^\dagger,a_{-k},b_k^\dagger,b_{-k}\}$  with two kind of quasiparticles  $\{\gamma_{k,1}^\dagger,\gamma_{-k,1},\gamma_{k,2}^\dagger,\gamma_{-k,2}\}$  as follows,

$$\begin{pmatrix} \gamma_{k,1}^{\dagger} \\ \gamma_{-k,1} \\ \gamma_{k,2}^{\dagger} \\ \gamma_{-k,2} \end{pmatrix} = \hat{U}_k \begin{pmatrix} a_k^{\dagger} \\ a_{-k} \\ b_k^{\dagger} \\ b_{-k} \end{pmatrix}, \tag{A3}$$

The obtained four eigenenergies  $\{\varepsilon_{k,j}\}$   $(j=1,\cdots,4)$  are the excitations in the artificially enlarged particlehole space where the positive (negative) ones denote the electron (hole) excitations. The ground state corresponds to the state in which all hole modes are occupied while the electron modes are vacant. The PHS indicates here that

$$\varepsilon_{k,1(2)} = \sqrt{\varsigma_k + (-1)^j \sqrt{\tau_k}} > 0,$$
  

$$\varepsilon_{k,4(3)} = -\varepsilon_{-k,1(2)} < 0.$$

The diagonal form of the Hamiltonian model,

$$\hat{H}_{k} = \frac{1}{2} \varepsilon_{k,1} \left( \gamma_{k,1}^{\dagger} \gamma_{k,1} - \gamma_{-k,1} \gamma_{-k,1}^{\dagger} \right) 
+ \frac{1}{2} \varepsilon_{k,2} \left( \gamma_{k,2}^{\dagger} \gamma_{k,2} - \gamma_{-k,2} \gamma_{-k,2}^{\dagger} \right) 
= \sum_{j=1}^{2} \varepsilon_{k,j} \left( \gamma_{k,j}^{\dagger} \gamma_{k,j} - \frac{1}{2} \right).$$
(A4)

On the other hand, we can use a basis in which the eigenstates of  $H_k$  are obtained as linear combinations of even-parity fermion states. Here we outline the connection between these two approaches. A general eigenstate is

$$|\psi_{m,k}\rangle = v_1^m |0\rangle + v_2^m a_k^{\dagger} a_{-k}^{\dagger} |0\rangle + v_3^m a_k^{\dagger} b_{-k}^{\dagger} |0\rangle + v_4^m a_{-k}^{\dagger} b_k^{\dagger} |0\rangle + v_5^m b_k^{\dagger} b_{-k}^{\dagger} |0\rangle + v_6^m a_k^{\dagger} a_{-k}^{\dagger} b_k^{\dagger} b_{-k}^{\dagger} |0\rangle,$$
(A5)

with  $m = 1, 2, \dots, 6$ . In other words, we introduce basis vectors for every k,

$$\begin{split} |\varphi_{1,k}\rangle &= |0\rangle, & |\varphi_{2,k}\rangle = a_k^\dagger a_{-k}^\dagger |0\rangle, \\ |\varphi_{3,k}\rangle &= a_k^\dagger b_{-k}^\dagger |0\rangle, & |\varphi_{4,k}\rangle = a_{-k}^\dagger b_k^\dagger |0\rangle, \\ |\varphi_{5,k}\rangle &= b_k^\dagger b_{-k}^\dagger |0\rangle, & |\varphi_{6,k}\rangle = a_k^\dagger a_{-k}^\dagger b_k^\dagger b_{-k}^\dagger |0\rangle. & \text{(A6)} \end{split}$$
 The subspace used in Eq. (A5) is six-dimensional which is due to the selected pairs from four modes. In this case,

$$\hat{H}_k = \Sigma_k^{\dagger} \hat{\Xi}_k \Sigma_k, \tag{A7}$$

where  $\hat{\Xi}_k$  can be written explicitly in terms of the matrix elements of  $\hat{M}_k$  in Eq. (A1):

$$\hat{\Xi}_{k} = \begin{pmatrix} M_{22} + M_{44} & M_{12} & M_{14} & -M_{32} & M_{34} & 0 \\ M_{21} & M_{11} + M_{44} & -M_{24} & -M_{31} & 0 & M_{34} \\ M_{41} & -M_{42} & M_{11} + M_{22} & 0 & M_{31} & -M_{32} \\ -M_{23} & -M_{13} & 0 & M_{33} + M_{44} & M_{24} & M_{14} \\ M_{43} & 0 & M_{13} & M_{42} & M_{22} + M_{33} & M_{12} \\ 0 & M_{43} & -M_{23} & M_{41} & M_{21} & M_{11} + M_{33} \end{pmatrix}.$$
(A8)

## Appendix B: To diagonalize a general Hamiltonian quadratic in fermions

The presented analytic method requires diagonalization of a general quadratic Hamiltonian of the form,

$$H = \sum_{i,j} \left\{ c_i^{\dagger} A_{ij} c_j + \frac{1}{2} \left( c_i^{\dagger} B_{ij} c_j^{\dagger} - c_i B_{ij}^* c_j \right) \right\}, (B1)$$

where  $c_i$  and  $c_i^{\dagger}$  are fermion annihilation and creation operators respectively. For system size N, A and B are both  $N \times N$  matrices. The requirement of translation-invariance implies that A and B are Toeplitz matrices, i.e.,  $A_{i+n,j+n} = A_{i,j}$  and  $B_{i+n,j+n} = B_{i,j}$  for any  $n \in \mathbb{N}$ . Hermiticity of H implies that A is a (possibly complex) Hermitian matrix and B is a (possibly complex) anti-

symmetric matrix. Finite-ranged interaction means that there exists a positive integer  $l_0$  such that  $A_{0,l}=B_{0,l}=0$  if  $l \ge l_0$ .

Such a spin-chain Hamiltonian is not invariant with respect to the reflection transformation  $R(\sigma_i^a) = \sigma_{-i}^a$  (a=x,y,z) when A is not a real matrix. One of the typical quantum spin chains with broken reflection symmetry is the Ising model with transverse magnetic field and Dzyaloshinskii-Moriya interaction (in the z-direction). Extra care should be taken that B matrix is not real in these cases.

Normally, people believe that  $\langle \sigma_i^x \sigma_j^y \rangle$  ( $\langle \sigma_i^y \sigma_j^x \rangle$ ) is zero due to the imaginary character of  $\sigma_j^y$  ( $\sigma_i^y$ ). Here we disprove this argument in our model due to its complex nature of Hamiltonian. Also, be aware that the relations between correlations where

$$\langle \sigma_0^z \sigma_r^z \rangle = \langle \sigma_0^z \rangle \langle \sigma_r^z \rangle - G_r G_{-r},$$
 (B2)

is not always valid. In this appendix we will show that this is not correct. Here

$$G_r = \langle B_0 A_r \rangle,$$
 (B3)

where

$$A_i \equiv c_i^{\dagger} + c_i, \quad B_i \equiv c_i^{\dagger} - c_i.$$
 (B4)

We can write

$$\sigma_i^x = A_i \prod_{j=1}^{i-1} A_j B_j,$$

$$\sigma_i^y = i B_i \prod_{j=1}^{i-1} A_j B_j,$$

$$\sigma_i^z = A_i B_i,$$
(B5)

and we have

$$\rho_{i,i+1}^{xx} = \langle B_i A_{i+1} \rangle, 
\rho_{i,i+1}^{yy} = -\langle A_i B_{i+1} \rangle, 
\rho_{i,i+1}^{zz} = \langle A_i B_i A_{i+1} B_{i+1} \rangle 
= \langle A_i B_i \rangle \langle A_{i+1} B_{i+1} \rangle - \langle A_i B_{i+1} \rangle \langle A_{i+1} B_i \rangle 
- \langle A_i A_{i+1} \rangle \langle B_i B_{i+1} \rangle.$$
(B6)

Generally speaking, they are claimed to obey the algebra irrespective of detailed eigenspectrum,

$${A_i, A_j} = 2\delta_{ij}, {B_i, B_j} = -2\delta_{ij}, {A_i, B_j} = 0. (B7)$$

However, one may be easily verified that it is not true. Take nearest neighbor sites for example, i.e., |j - i| = 1 and one has

$$\langle A_i A_{i+1} \rangle = -i \langle \sigma_i^y \sigma_{i+1}^x \rangle, \langle B_i B_{i+1} \rangle = -i \langle \sigma_i^x \sigma_{i+1}^y \rangle,$$
(B8)

In what follows we concentrate on the correlations between the nearest neighbor spins. By straightforward calculation it is found that the nearest neighbor spin correlation function has the form  $\langle \sigma_i^x \sigma_{i+1}^y \rangle = -\langle \sigma_i^y \sigma_{i+1}^x \rangle = i \langle B_i B_{i+1} \rangle$ , so element  $z_1$  for the nearest neighbor spins is always a real number and  $z_2$  may be a complex number depending on which phase the system is in.

Therefore, the two-qubit density matrix reduces to an X-state,

$$\rho_{ij} = \begin{pmatrix} u^{+} & 0 & 0 & z_{1} \\ 0 & w^{+} & z_{2} & 0 \\ 0 & z_{2}^{*} & w^{-} & 0 \\ z_{1}^{*} & 0 & 0 & u^{-} \end{pmatrix},$$
(B9)

with

$$\begin{split} u^{\pm} &= \frac{1}{4} (1 \pm \langle \sigma_i^z \rangle \pm \langle \sigma_j^z \rangle + \langle \sigma_i^z \sigma_j^z \rangle), \\ z_1 &= \frac{1}{4} (\langle \sigma_i^x \sigma_j^x \rangle - \langle \sigma_i^y \sigma_j^y \rangle - i \langle \sigma_i^x \sigma_j^y \rangle - i \langle \sigma_i^y \sigma_j^x \rangle), \\ z_2 &= \frac{1}{4} (\langle \sigma_i^x \sigma_j^x \rangle + \langle \sigma_i^y \sigma_j^y \rangle + i \langle \sigma_i^x \sigma_j^y \rangle - i \langle \sigma_i^y \sigma_j^x \rangle), \\ \omega^{\pm} &= \frac{1}{4} (1 \pm \langle \sigma_i^z \rangle \mp \langle \sigma_j^z \rangle - \langle \sigma_i^z \sigma_j^z \rangle). \end{split}$$

When the system is translation invariant, we obtain  $\langle \sigma_i^z \rangle = \langle \sigma_j^z \rangle$  ( $\forall i, j$ ) such that  $\omega^+ = \omega^-$ . This missing of terms like  $\langle \sigma_i^x \sigma_j^y \rangle$ ,  $\langle \sigma_i^y \sigma_j^x \rangle$  commonly exist in Ref. [78] or a negligence taking  $\langle c_i^\dagger c_{i+1}^\dagger \rangle = 0$  for granted in calculations of  $\langle \sigma_i^z \sigma_j^z \rangle$  [27].

Finally, by a numerical calculation we confirm that

$$\begin{split} \langle \sigma_i^x \sigma_{i+1}^y \rangle &= \langle \sigma_i^y \sigma_{i+1}^x \rangle, \\ \langle \sigma_i^z \sigma_{i+1}^z \rangle &= \langle \sigma_i^z \rangle^2 \\ &- \langle \sigma_i^x \sigma_{i+1}^x \rangle \langle \sigma_i^y \sigma_{i+1}^y \rangle + \langle \sigma_i^x \sigma_{i+1}^y \rangle \langle \sigma_i^y \sigma_{i+1}^x \rangle. \end{split}$$

- Z. Nussinov and J. van den Brink, Rev. Mod. Phys. 87, 1 (2015).
- [2] W. Brzezicki, J. Dziarmaga, and A. M. Oleś, Phys. Rev. B 75, 134415 (2007); W. Brzezicki and A. M. Oleś, Acta Phys. Polon. A 115, 162 (2009).
- [3] J. P. Goff, D. A. Tennant, and S. E. Nagler, Phys. Rev. B 52, 15992 (1995).
- [4] T. Masuda, A. Zheludev, A. Bush, M. Markina, and A. Vasiliev, Phys. Rev. Lett. 92, 177201 (2004).
- [5] A. Rusydi, I. Mahns, S. Muller, M. Rubhausen, S. Park,

- Y. J. Choi, C. L. Zhang, S.-W. Cheong, S. Smadici, P. Abbamonte, M. V. Zimmermann, and G. A. Sawatzky, Appl. Phys. Lett. **92**, 262506 (2008).
- [6] L. Capogna, M. Reehuis, A. Maljuk, R. K. Kremer, B. Ouladdiaf, M. Jansen, and B. Keimer, Phys. Rev. B 82, 014407 (2010).
- [7] M. Suzuki, Prog. Theor. Phys. 46, 1337 (1971).
- [8] X. Peng, J. Zhang, J. Du, and D. Suter, Phys. Rev. Lett. 103, 140501 (2009).
- [9] C. H. Tseng, S. Somaroo, Y. Sharf, E. Knill, R. Laflamme, T. F. Havel, and D. G. Cory, Phys. Rev. A 61, 012302 (1999).
- [10] J. Zhang, X. Peng, and D. Suter, Phys. Rev. A 73, 062325 (2006).
- [11] V. Derzhko, O. Derzhko, and J. Richter, Phys. Rev. B 83, 174428 (2011).
- [12] D. Eloy and J. C. Xavier, Phys. Rev. B 86, 064421 (2012).
- [13] I. Titvinidze and G. I. Japaridze, Eur. Phys. J. B 32, 383 (2003).
- [14] M. Topilko, T. Krokhmalskii, O. Derzhko, and V. Ohanyan, Eur. Phys. J. B 85, 278 (2012).
- [15] O. Menchyshyn, V. Ohanyan, T. Verkholyak, T. Krokhmalskii, and O. Derzhko, Phys. Rev. B 92, 184427 (2015).
- [16] T. Krokhmalskii, O. Derzhko, J. Stolze, and T. Verkholyak, Phys. Rev. B 77, 174404 (2008).
- [17] P. Lou, W.-C. Wu, and M.-C. Chang, Phys. Rev. B 70, 064405 (2004).
- [18] W. W. Cheng and J.-M. Liu, Phys. Rev. A 82, 012308 (2010).
- [19] A. A. Zvyagin, Phys. Rev. B 80, 014414 (2009).
- [20] H. L. Lian and D. P. Tian, Phys. Lett. A 375, 3604 (2011).
- [21] W. W. Cheng, C. J. Shan, Y. X. Huang, T. K. Liu, and H. Li, Physica B 405, 4821 (2010).
- [22] G. Zhang and Z. Song, Phys. Rev. Lett. 115, 177204 (2015).
- [23] Yan-Chao Li and Hai-Qing Lin, Phys. Rev. A 83, 052323 (2011).
- [24] HanLi Lian, Physica B 406, 4278 (2011).
- [25] W. W. Cheng and J.-M. Liu, Phys. Rev. A 81, 044304 (2010).
- [26] Ping Lou, Phys. Rev. B 72, 064435 (2005).
- [27] S. Lei and P. Tong, Physica B 463, 1 (2015).
- [28] Xiaoxian Liu, Ming Zhong, Hui Xu and Peiqing Tong, J. Stat. Mech. P01003 (2012).
- [29] A. Kopp and S. Chakravarty, Nat. Phys. 1, 53 (2005).
- [30] Y. Niu, S. B. Chung, C.-H. Hsu, I. Mandal, S. Raghu, and S. Chakravarty, Phys. Rev. B 85, 035110 (2012).
- [31] Atanu Rajak and Uma Divakaran, J. Stat. Mech. P04023 (2007).
- [32] Y. L. Dong, T. Neupert, R. Chitra, and S. Schmidt Phys. Rev. B 94, 035441 (2016).
- [33] E. Fradkin and L. Susskind, Phys. Rev. D 17, 2637 (1978).
- [34] M. Mochizuki, N. Furukawa, and N. Nagaosa, Phys. Rev. Lett. 105, 037205 (2010); Phys. Rev. B 84, 144409 (2011).
- [35] W.-L. You, P. Horsch, and A. M. Oleś, Phys. Rev. B 89, 104425 (2014).
- [36] W.-L. You, G.-H. Liu, P. Horsch, and A. M. Oleś, Phys. Rev. B 90, 094413 (2014).
- [37] W.-L. You, Y.-C. Qiu, and A. M. Oleś, Phys. Rev. B 93,

- 214417 (2016).
- [38] Q.-C Wu, W.-H Ni, and W.-L. You, J. Phys.: Condens. Matter 29, 225804 (2017).
- [39] J. E. Hirsch and G. F. Mazenko, Phys. Rev. B 19, 2656 (1979).
- [40] J. K. Pachos and M. B. Plenio, Phys. Rev. Lett. 93, 056402 (2004).
- [41] Y.-C. Qiu, Q.-Q. Wu and W.-L. You, J. Phys.: Condens. Matter 28, 496001 (2016).
- [42] R. Steinigeweg and W. Brenig, Phys. Rev. B 93, 214425 (2016).
- [43] X. Zotos, F. Naef, and P. Prelovšek, Phys. Rev. B 55, 11029 (1997).
- [44] T. Antal, Z. Rácz, and L. Sasvári, Phys. Rev. Lett. 78, 167 (1997).
- [45] Y. Salathé, M. Mondal, M. Oppliger, J. Heinsoo, P. Kurpiers, A. Potocnik, A. Mezzacapo, U. Las Heras, L. Lamata, E. Solano, S. Filipp, and A. Wallraff, Phys. Rev. X 5, 021027 (2015).
- [46] A. Mezzacapo, L. Lamata, S. Filipp, and E. Solano, Phys. Rev. Lett. 113, 050501 (2014).
- [47] C.-E. Bardyn and A. İmamoğlu, Phys. Rev. Lett. 109, 253606 (2012).
- [48] E. H. Lieb, T. Schulz, D.Mattis, Ann. Phys. (N.Y.) 16, 407 (1961).
- [49] S. Katsura, Phys. Rev. 127, 1508 (1962).
- [50] E. Barouch and B. M. McCoy, Phys. Rev. A 2, 1075 (1970); 3, 786 (1971).
- Y. Xiong and P. Tong, New J. Phys. 17, 013017 (2015);
   X. Wang, T. Liu, and Y. Xiong and P. Tong, Phys. Rev. A 92, 012116 (2015).
- [52] R. Jafari and H. Johannesson, Phys. Rev. Lett. 118, 015701 (2017).
- [53] L. Cincio, J. Dziarmaga, and A. M. Oleś, Phys. Rev. B 82, 104416 (2010).
- [54] O. Derzhko, in: Condensed Matter Physics in the Prime of the 21st Century. Phenomena, Materials, Ideas, Methods, edited by J. Jedrzejewski (World Scientific, Singapore, 2008).
- [55] W.-L. You and G.-S. Tian, Phys. Rev. B 78, 184406 (2008).
- [56] C.-K. Chiu, J. C. Y. Teo, A. P. Schnyder, and S. Ryu, Rev. Mod. Phys. 88, 035005 (2016).
- [57] A. Yu. Kitaev, Phys.-Usp. (Suppl.) 44, 131 (2001).
- [58] P. Ghosh, J. D. Sau, S. Tewari, and S. Das Sarma, Phys. Rev. B 82, 184525 (2010).
- [59] D. C. Dender, P. R. Hammar, D. H. Reich, C. Broholm, and G. Aeppli, Phys. Rev. Lett. 79, 1750 (1997).
- [60] Y. Kono, T. Sakakibara, C. P. Aoyama, C. Hotta, M. M. Turnbull, C. P. Landee, and Y. Takano, Phys. Rev. Lett. 114, 037202 (2015).
- [61] T. Liang, S. M. Koohpayeh, J. W. Krizan, T. M. Mc-Queen, R. J. Cava, and N. P. Ong, Nature Commun. 6, 7611 (2015).
- [62] Ke-Wei Sun and Qing-Hu Chen, Phys. Rev. B 80, 174417 (2009).
- [63] M. Motamedifar, S. Mahdavifar, S. F. Shayesteh, and S. Nemati, Phys. Scr. 88, 015003 (2013).
- [64] E. Eriksson and H. Johannesson, Phys. Rev. B 79, 224424 (2009).
- [65] M. Imada, F. F. Assaad, H. Tsunetsugu, and Y. Motome, in: *Physics and Chemistry of Transition Metal Ox*ides, edited by H. Fukuyama and N. Nagaosa (Springer,

- Berlin, 1999), p. 120-135.
- [66] L. Huijse, B. Bauer, and E. Berg, Phys. Rev. Lett. 114, 090404 (2015).
- [67] A. Osterloh, L. Amico, G. Falci, and R. Fazio, Nature 416, 608 (2002).
- [68] Shi-Jian Gu, Shu-Sa Deng, You-Quan Li, and Hai-Qing Lin, Phys. Rev. Lett. 93, 086402 (2004).
- [69] P. Zanardi, H. T. Quan, X. Wang, and C. P. Sun, Phys. Rev. A 75, 032109 (2007).
- [70] W.-L. You, Y.-W. Li, and S.-J. Gu, Phys. Rev. E 76, 022101 (2007).
- [71] L. Campos Venuti and P. Zanardi, Phys. Rev. Lett. 99, 095701 (2007).
- [72] Shi-Jian Gu, Int. J. Mod. Phys. B 24, 4371 (2010).
- [73] M. Miyaji, T. Numasawa, N. Shiba, T. Takayanagi, and K. Watanabe, Phys. Rev. Lett 115, 261602 (2015).
- [74] M.-F. Yang, Phys. Rev. B 76, 180403 (2007).
- [75] B. Wang, M. Feng, and Z.-Q. Chen, Phys. Rev. A 81,

- 064301 (2010).
- [76] G. Sun, A. K. Kolezhuk, and T. Vekua, Phys. Rev. B 91, 014418 (2015).
- [77] W.-L. You and L. He, J. Phys.: Condens. Matter 27, 205601 (2015).
- [78] B.-Q. Liu, B. Shao, J.-G. Li, J. Zou, and L.-Ao Wu, Phys. Rev. A 83, 052112 (2011).
- [79] Jin-Jun Chen, Jian Cui, Yu-Ran Zhang, and Heng Fan, Phys. Rev. A 94, 022112 (2016).
- [80] R. Dillenschneider, Phys. Rev. B 78, 224413 (2008).
- [81] M. S. Sarandy, Phys. Rev. A 80, 022108 (2009).
- [82] T. Werlang, C. Trippe, G. A. P. Ribeiro, and G. Rigolin, Phys. Rev. Lett. 105, 095702 (2010).
- [83] H. Ollivier and W. H. Zurek, Phys. Rev. Lett. 88, 017901 (2001).
- [84] W. K. Wootters, Phys. Rev. Lett. 80, 2245 (1998).